

- (8) S. A. Bezman, M. R. Churchill, J. A. Osborn, and J. Wormald, *J. Am. Chem. Soc.*, **93**, 2063 (1971); M. R. Churchill, S. A. Bezman, J. A. Osborn, and J. Wormald, *Inorg. Chem.*, **11**, 1818 (1972).
- (9) M. R. Churchill and S. W.-Y. Ni, *J. Am. Chem. Soc.*, **95**, 2150 (1973).
- (10) M. R. Churchill, S. W.-Y. Ni, N. Chang, M. L. Berch, and A. Davison, *J. Chem. Soc., Chem. Commun.*, 691 (1973); M. R. Churchill and S. W.-Y. Ni, *Inorg. Chem.*, **13**, 2413 (1974).
- (11) (a) M. R. Churchill, B. G. DeBoer, F. J. Rotella, E. W. Abel, and R. J. Rowley, *J. Am. Chem. Soc.*, **97**, 7158 (1975); (b) M. R. Churchill, B. G. DeBoer, and F. J. Rotella, *Inorg. Chem.*, **15**, 1843 (1976).
- (12) M. R. Churchill, B. G. DeBoer, J. R. Shapley, and J. B. Keister, *J. Am. Chem. Soc.*, **98**, 2357 (1976).
- (13) J. R. Shapley, J. B. Keister, M. R. Churchill, and B. G. DeBoer, *J. Am. Chem. Soc.*, **97**, 4145 (1975).
- (14) E. R. Corey and L. F. Dahl, *Inorg. Chem.*, **1**, 521 (1962).
- (15) M. R. Churchill and B. G. DeBoer, *Inorg. Chem.*, **12**, 525 (1973).
- (16) The largest faces were {010} and {001}; other faces were {011} and {0 $\bar{1}$ 1} (which clip two corners of the prism), {11 $\bar{2}$ }, {1 $\bar{1}$ 2}, {110}, and { $\bar{1}$ 10} which define a square-pyramidal end at the "top" of the prism, and { $\bar{1}$ 10}, { $\bar{1}$ 11}, and { $\bar{1}$ 11} which approximate the broken "bottom" end of the prism.
- (17) D. T. Cromer and J. B. Mann, *Acta Crystallogr., Sect. A*, **24**, 321 (1968).
- (18) D. T. Cromer and D. Liberman, *J. Chem. Phys.*, **53**, 1891 (1970).
- (19) W. H. Zachariasen, *Acta Crystallogr.*, **16**, 1139 (1963); **23**, 558 (1967); A. C. Larson in "Crystallographic Computing", F. R. Ahmed, Ed., Munksgaard, Copenhagen, 1970, p 251 ff.
- (20) Esd's on individual measurements are enclosed by parentheses (see footnote a to Table II). Esd's on averaged values are enclosed by brackets (see footnote b to Table IV).
- (21) R. Mason and A. I. M. Rae, *J. Chem. Soc. A*, 778 (1968).

Contribution from the Max-Planck-Institut für Kohlenforschung,
4330 Mülheim a.d. Ruhr, West Germany

Bonding of Aromatic Hydrocarbons to Ni(0). Structure of Bistricyclohexylphosphine(1,2- η^2 -anthracene)nickel(0)-Toluene

D. J. BRAUER and C. KRÜGER*

Received July 8, 1976

AIC60503N

The crystal structure of bistricyclohexylphosphine(1,2- η^2 -anthracene)nickel(0)-toluene has been determined from 4743 x-ray data with $I \geq 2\sigma(I)$. The compound crystallizes in the triclinic system with unit cell dimensions $a = 9.8620$ (9), $b = 13.956$ (1), $c = 19.755$ (2) Å, $\alpha = 93.398$ (8), $\beta = 91.872$ (9), and $\gamma = 110.166$ (8)°. The crystals have a calculated density of 1.16 g/cm³ for $Z = 2$ in the space group $P\bar{1}$. The structure was refined by block diagonal least-squares methods with anisotropic temperature factors for all nonhydrogen atoms and isotropic temperature factors for the anthracenic and cyclohexyl hydrogen atoms. The final R value is 0.039. The crystals consist of distinct, monomeric bistricyclohexylphosphine(1,2- η^2 -anthracene)nickel(0) molecules, which are separated from the two independent, disordered toluene molecules by van der Waals distances. The bonds formed by the Ni atom are Ni-P(1), 2.227 (1) Å, Ni-P(2), 2.241 (1) Å, Ni-C(1), 2.060 (4) Å, and Ni-C(2), 1.993 (4) Å. The P(1)-Ni-P(2) angle is 118.3 (1)°. The C(1)-C(2) bond of anthracene is lengthened 0.047 (6) Å by coordination. The substituent planes of C(1) and C(2) are bent back 19 (1)° from the Ni atom. The C(1)-C(2) vector is rotated 22.0° out of the plane of Ni, P(1), P(2). The latter as well as other distortions are discussed in terms of the tight packing of ligands about the metal atom. Evidence for partial fixation of single and double bonds in the anthracene moiety is presented. From this observation a model based on a minimized loss of arene resonance energy is formulated and used to predict structures of other 1,2-dihaptoarene transition metal complexes and their relative stabilities.

Introduction

Recently the synthesis of a number of [(C₆H₁₁)₂P(CH₂)_n]₂Ni ($n = 2, 3$) and [(C₆H₁₁)₃P]₂Ni-(TCP)₂Ni—complexes of benzene, naphthalene, phenanthrene, anthracene, and tetracene have been reported. The benzene and, to a lesser extent, naphthalene containing compounds react with hydrogen to form a nickel hydride complex. While spectroscopic and potentiometric measurements indicated that the aromatic ligands probably interact with the nickel atom, no detailed structural information could be presented.¹

Because these compounds belong to a new class of nickel complexes, we were interested in this stereochemistry. Since NMR methods were hindered by the low solubility and dissociation of the compounds,¹ recourse to single-crystal x-ray diffraction techniques was obvious. Attempts to analyze chelate phosphine complexes proved fruitless due to poor crystal quality. Finally good crystals of (TCP)₂(C₁₄H₁₀)Ni, which contain toluene solvent, were kindly supplied by Dr. Jonas of this institute. We wish to report the results of this x-ray structural investigation.

Experimental Section

A crystal of (TCP)₂(C₁₄H₁₀)Ni·C₆H₅CH₃ of dimensions 0.325 × 0.15 × 0.225 mm was mounted in a glass capillary under argon. Weissenberg and precession photographs indicated that the crystal belongs to the triclinic system. No higher symmetry was revealed by a reduced cell calculation.² The crystal was transferred to an automated CAD-4 diffractometer, which was equipped with a

molybdenum source and a graphite monochromator.

An orientation matrix was calculated before data collection from the setting angles of 15 centered reflections. At the end of data collection, precise unit cell constants were obtained by a least-squares technique employing the Bragg angles (Mo K α 0.71069 Å) of 89 reflections with $12^\circ < 2\theta < 35^\circ$. The unit cell dimensions are $a = 9.8620$ (9),³ $b = 13.956$ (1), $c = 19.755$ (2) Å, $\alpha = 93.398$ (8), $\beta = 91.872$ (9), and $\gamma = 110.166$ (8)°. The calculated density is 1.16 g/cm³ for $Z = 2$. θ scans of several strong reflections indicated that the crystalline quality was satisfactory. One hemisphere ($hkl, \bar{h}kl, h\bar{k}l, \bar{h}k\bar{l}$, $0.5^\circ < 2\theta(\text{Mo K}\alpha) < 25.0^\circ$) of data was collected by the $\theta/2\theta$ scan technique. Before each intensity measurement a fast scan of the reflection at 20°/min was used to determine the final scanning speed. Moving crystal-moving counter background scans were made by scanning a quarter of the peak width before the start and also after the end of each peak scan. The check reflections 500, 040, and 004 were remeasured after collection of 250 data. These reflections were used to check on the centering and stability of the crystal and diffractometer. The variation of the intensities of the check reflections was less than 7%. A total of 8930 data were collected.

The intensity data were corrected for check reflection fluctuation and reduced to $|F_o|$'s. The fact that no absorption correction ($\mu = 4.8 \text{ cm}^{-1}$) was applied causes relative errors of less than 5% in the intensities. Multiply measured reflections were averaged to yield 8911 data. Of these, 4734 obeyed the condition $I \geq 2\sigma(I)$ and were considered "observed". Here $I = K[P - 2(\text{BG1} + \text{BG2})]$ and $\sigma(I) = K(P + 4(\text{BG1} + \text{BG2}))^{1/2}$, where P is the peak intensity, BG1 and BG2 are the background intensities, and K is a constant which depends on the scanning speed. Each "observed" reflection was assigned a standard deviation $\sigma(|F_o|)$, where $\sigma(|F_o|) = (\sigma^2(I) + (0.04I)^2)^{1/2}/2F$.

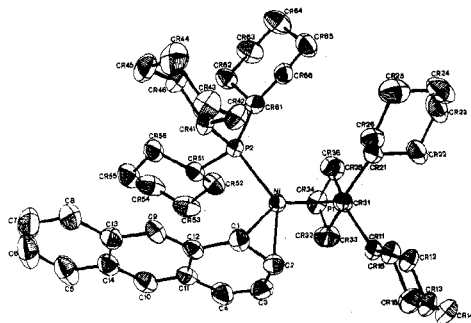


Figure 1. Stereodrawing of $(TCP)_2C_{14}H_{10}Ni$ with 50% probability thermal ellipsoids. Hydrogen atoms have been omitted.

Solution and Refinement of the Crystal Structure. The structure was solved by the heavy atom method. Positions for a Ni atom and two P atoms were obtained from an E 's sharpened Patterson map. The agreement factors based on these three atoms were $R = \sum \Delta / \sum |F_o| = 0.484$ and $R_w = [\sum w\Delta^2 / \sum w|F_o|^2] = 0.477$, where $\Delta = \|F_o| - |F_c||$ and $w = 1/\sigma^2(|F_o|)$ for "observed" reflections and $w = 0$ for "unobserved" reflections. Positions for all anthracene and cyclohexyl carbon atoms were obtained from a subsequent Fourier map. The agreement factors before refinement of the structure were $R = 0.278$ and $R_w = 0.317$.

The structure was refined isotropically by full matrix least squares and anisotropically by block diagonal least-squares techniques. The function minimized was $\sum w\Delta^2$. Relativistic Hartree-Fock scattering factors^{4a} were used for Ni, P, and C, and the best spherical scattering factors^{4b} were used for H. The real and imaginary components of the anomalous scattering factors of Ni and P⁵ were included in the structure factor calculation. The weights of the "observed" reflections in the block diagonal least-squares refinement were defined as $1/[\sigma^2(|F_o|) + (0.02|F_o|)^2]$.

Three cycles of isotropic least-squares refinement yielded $R = 0.131$ and $R_w = 0.200$. The largest peaks in a difference Fourier map were near two centers of inversion. These peaks had heights of 0.9–2.8 $e/\text{\AA}^3$, which may be compared to the heights of the previously found carbon atoms in this structure, 3.6–7.2 $e/\text{\AA}^3$. These peaks were presumed to be carbon atoms of two disordered toluene molecules. Since most of these peaks were elongated, five cycles of anisotropic refinement were employed, $R = 0.120$ and $R_w = 0.190$, before the following disorder model for the toluene molecules was chosen:

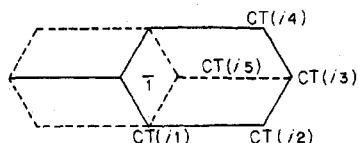


Figure 2. A perspective drawing of the $(C_{14}H_{10})Ni(PC_3)_2$ part of the molecule with arbitrary thermal ellipsoids.

III and IV, respectively. The numbering scheme is defined in Figure 1 for the nonhydrogen atoms of the $(TCP)_2(C_{14}H_{10})Ni$ portion of the structure; that for the toluene species is given in the above sketch. The hydrogen atoms are numbered after the carbon atoms to which they are attached.

Reliability of Derived Parameters

As an internal check on the least-squares standard deviations, we examined the distribution of C–H bond lengths. The 76 unique distances vary from 0.86 (4) to 1.07 (4) \AA , the average value is 0.97 \AA .⁶ The estimated standard deviation of an individual observation, as defined by $(\sum_i^n (l_i - \bar{l})^2 / (n - 1))^{1/2}$, is $\pm 0.05 \text{\AA}$. Using variances derived during least-squares refinement of the coordinates of C and H atoms, we obtained estimates of the standard deviations (average 0.036 \AA) of the C–H bond lengths. The difference in these estimates indicates that either the C–H distances do not have a common mean or that the least-squares σ 's are about 50% too low. We feel that the latter argument is more likely to be true in this case.

Description and Discussion of the Crystal Structure

Crystals of $(TCP)_2(C_{14}H_{10})Ni-C_6H_5CH_3$ consist of distinct monomeric nickel complexes and two crystallographically independent toluene molecules, which are disordered about inversion symmetry sites. The intermolecular contacts are normal, the shortest being H(16A)–H(34B) ($x - 1, y, z$), 2.39 (5) \AA .

In space group $P\bar{1}$, the toluene entities would not have to be disordered. We did not attempt a refinement in $P\bar{1}$ for three reasons. First, no unusually short contacts are formed by the toluene carbon atoms, the shortest is CT(22)–C(2) ($1 + x, y, z$), 3.59 (2) \AA ; therefore, cavities occupied by toluene molecules are sufficiently large to allow disordering of these atoms. Second, the nickel complex portion, including hydrogen atoms, refined well. From this observation we conclude that these parts of the crystal obey $P\bar{1}$ crystallographic symmetry satisfactorily. Third, the $P\bar{1}$ structure fits the intensity data reasonably well as is indicated by the final agreement factors. The derived toluene C–C bond lengths vary from 1.25 (2) to

Thus independent carbon atoms of each unique, disordered toluene species could be described by five sets of positional parameters. The occupancies of CT(i 2), CT(i 4), and CT(i 5) ($i = 1, 2$) were taken as 0.5.

Then the positions of the anthracenic and cyclohexyl hydrogen atoms were calculated (sp^2 or sp^3 hybridization, C–H = 0.95 \AA). These positions were confirmed by difference Fourier densities between 0.1 and 0.8 $e/\text{\AA}^3$ in nearly each of the 76 cases. No attempt was made to locate the toluene hydrogen atoms. Six cycles of anisotropic refinement (toluene C atoms isotropic and H atoms not refined) gave 0.054 and 0.062 for R and R_w , respectively. Then all nonhydrogen atoms were refined anisotropically and the H atoms were refined isotropically for 16 cycles. The final agreement factors were $R = 0.039$ and $R_w = 0.046$ for 4734 observations and 872 parameters.

On the final cycle the largest values of the shift over error ratio were less than 0.20 and 0.44 for positional parameters of an ordered and disordered atom, respectively. The largest value of this ratio for a thermal parameter was 0.79 for $U(2,2)$ of the nickel atom, but generally this factor was lower than 0.1 for the remaining atoms.

The function $(w\Delta^2)$ was plotted against $\langle |F_o| \rangle$, $\sin \theta / \lambda$, and the reflection indices. These plots were interpreted as implying that no improvement in the refinement would be obtained by modifying the weighting scheme. The final value of the error of fit is 1.15. The positional and thermal parameters for the nonhydrogen atoms are given in Table I. The hydrogen atom parameters are listed in Table II. Selected bond distances and bond angles are contained in Tables

Table I. Final Atomic Coordinates ($\times 10^4$) and Final Thermal Parameters ($\times 10^3$) and Their Standard Deviations

Atom	x	y	z	U_{11}	U_{22}	U_{33}	U_{12}	U_{13}	U_{23}
N(1)	453.7 (5)	1686.1 (4)	3025.2 (2)	30.8 (2)	31.8 (3)	32.3 (2)	9.3 (2)	3.1 (2)	0.3 (2)
P(1)	2100.3 (10)	3103.1 (7)	3520.1 (5)	29.3 (5)	33.6 (6)	33.7 (5)	11.4 (4)	3.1 (4)	-0.8 (4)
P(2)	544.5 (10)	1336.4 (7)	1909.5 (5)	29.7 (5)	33.0 (5)	31.8 (5)	10.9 (4)	2.3 (4)	1.4 (4)
C(1)	-1486 (4)	602 (3)	3232 (2)	37 (2)	40 (2)	50 (2)	12 (2)	8 (2)	4 (2)
C(2)	-560 (5)	1027 (3)	3823 (2)	63 (3)	42 (2)	43 (2)	8 (2)	20 (2)	3 (2)
C(3)	251 (5)	442 (3)	4086 (2)	67 (3)	59 (3)	42 (3)	3 (2)	-6 (2)	9 (2)
C(4)	78 (5)	-512 (3)	3827 (2)	65 (3)	53 (3)	62 (3)	15 (2)	-12 (2)	15 (2)
C(5)	-2588 (5)	-3544 (3)	2254 (3)	72 (3)	43 (3)	102 (4)	15 (2)	27 (3)	2 (3)
C(6)	-3586 (6)	-3979 (4)	1739 (3)	82 (4)	51 (3)	103 (4)	-2 (3)	27 (3)	-27 (3)
C(7)	-4389 (6)	-3434 (4)	1461 (3)	75 (4)	68 (3)	69 (3)	-15 (3)	4 (3)	-16 (3)
C(8)	-4186 (5)	-2467 (3)	1705 (2)	60 (3)	52 (3)	59 (3)	-6 (2)	3 (2)	6 (2)
C(9)	-2894 (4)	-962 (3)	2506 (2)	36 (2)	34 (2)	56 (3)	6 (2)	7 (2)	8 (2)
C(10)	-1254 (5)	-2029 (3)	3041 (2)	59 (3)	44 (3)	62 (3)	22 (2)	14 (2)	16 (2)
C(11)	-985 (4)	-1019 (3)	3289 (2)	44 (2)	40 (2)	43 (2)	11 (2)	9 (2)	13 (2)
C(12)	-1807 (4)	-461 (3)	2998 (2)	34 (2)	35 (2)	41 (2)	8 (2)	11 (2)	9 (2)
C(13)	-3153 (4)	-1977 (3)	2244 (2)	44 (2)	43 (2)	48 (2)	2 (2)	14 (2)	8 (2)
C(14)	-2313 (4)	-2524 (3)	2521 (2)	53 (3)	39 (2)	54 (3)	9 (2)	20 (2)	5 (2)
CR(11)	1794 (4)	3305 (3)	4449 (2)	34 (2)	35 (2)	36 (2)	10 (2)	2 (2)	-1 (2)
CR(12)	3044 (4)	4011 (3)	4927 (2)	40 (2)	52 (3)	43 (2)	15 (2)	-3 (2)	-7 (2)
CR(13)	2603 (4)	3925 (3)	5662 (2)	49 (3)	60 (3)	40 (2)	13 (2)	-8 (2)	-14 (2)
CR(14)	1252 (5)	4173 (3)	5770 (2)	64 (3)	65 (3)	38 (2)	26 (2)	6 (2)	-8 (2)
CR(15)	14 (4)	3516 (3)	5288 (2)	49 (3)	59 (3)	49 (3)	23 (2)	7 (2)	-1 (2)
CR(16)	441 (4)	3598 (3)	4555 (2)	42 (2)	43 (2)	39 (2)	15 (2)	0 (2)	-3 (2)
CR(21)	2190 (4)	4298 (3)	3115 (2)	39 (2)	41 (2)	40 (2)	19 (2)	9 (2)	4 (2)
CR(22)	3174 (5)	5324 (3)	3457 (2)	57 (3)	38 (2)	71 (3)	10 (2)	14 (2)	6 (2)
CR(23)	3284 (6)	6195 (3)	3009 (3)	101 (4)	40 (3)	99 (4)	17 (3)	41 (3)	15 (3)
CR(24)	1818 (7)	6247 (4)	2823 (3)	132 (5)	61 (3)	93 (4)	63 (3)	49 (4)	33 (3)
CR(25)	823 (6)	5239 (4)	2489 (2)	96 (4)	94 (4)	64 (3)	69 (3)	21 (3)	22 (3)
CR(26)	701 (4)	4353 (3)	2929 (2)	52 (3)	54 (3)	47 (2)	30 (2)	6 (2)	9 (2)
CR(31)	4034 (4)	3204 (3)	3573 (2)	32 (2)	36 (2)	40 (2)	12 (2)	1 (2)	-1 (2)
CR(32)	4236 (4)	2315 (3)	3927 (2)	46 (2)	51 (3)	52 (3)	23 (2)	5 (2)	9 (2)
CR(33)	5840 (5)	2432 (4)	3999 (2)	53 (3)	68 (3)	66 (3)	29 (2)	-7 (2)	5 (2)
CR(34)	6530 (4)	2538 (3)	3328 (2)	39 (3)	74 (3)	69 (3)	30 (2)	-2 (2)	-8 (2)
CR(35)	6333 (4)	3410 (3)	2970 (2)	39 (2)	59 (3)	57 (3)	18 (2)	11 (2)	-4 (2)
CR(36)	4734 (4)	3291 (3)	2886 (2)	38 (2)	58 (3)	46 (2)	25 (2)	3 (2)	4 (2)
CR(41)	-1264 (4)	1037 (3)	1454 (2)	33 (2)	36 (2)	38 (2)	8 (2)	1 (2)	-3 (2)
CR(42)	-1996 (4)	1804 (3)	1687 (2)	40 (2)	62 (3)	39 (2)	23 (2)	-0 (2)	-8 (2)
CR(43)	-3585 (4)	1415 (3)	1444 (2)	38 (2)	70 (3)	62 (3)	23 (2)	-1 (2)	-1 (2)
CR(44)	-3769 (5)	1199 (4)	682 (2)	39 (3)	77 (3)	75 (3)	21 (2)	-19 (2)	-4 (3)
CR(45)	-3004 (5)	470 (3)	439 (2)	54 (3)	65 (3)	49 (3)	11 (2)	-16 (2)	-8 (2)
CR(46)	-1413 (4)	876 (3)	678 (2)	41 (2)	53 (3)	40 (2)	15 (2)	-2 (2)	-4 (2)
CR(51)	900 (4)	102 (3)	1853 (2)	43 (2)	39 (2)	44 (2)	17 (2)	12 (2)	7 (2)
CR(52)	2453 (5)	285 (3)	2129 (2)	53 (3)	55 (3)	69 (3)	27 (2)	5 (2)	11 (2)
CR(53)	2707 (5)	-731 (4)	2197 (3)	70 (3)	85 (4)	82 (4)	48 (3)	11 (3)	30 (3)
CR(54)	2348 (6)	-1390 (4)	1539 (3)	116 (4)	78 (4)	83 (4)	70 (3)	44 (3)	32 (3)
CR(55)	795 (6)	-1601 (3)	1290 (2)	96 (4)	46 (3)	77 (3)	34 (3)	32 (3)	2 (2)
CR(56)	475 (5)	-614 (3)	1205 (2)	67 (3)	41 (2)	53 (3)	23 (2)	17 (2)	-2 (2)
CR(61)	1914 (4)	2228 (3)	1391 (2)	32 (2)	40 (2)	43 (2)	10 (2)	2 (2)	8 (2)
CR(62)	2368 (4)	1837 (3)	719 (2)	52 (3)	49 (3)	53 (3)	20 (2)	21 (2)	15 (2)
CR(63)	3623 (5)	2678 (4)	448 (2)	54 (3)	79 (3)	72 (3)	24 (3)	33 (2)	29 (3)
CR(64)	3276 (5)	3637 (4)	355 (3)	67 (3)	68 (3)	85 (4)	13 (3)	32 (3)	35 (3)
CR(65)	2799 (5)	4023 (3)	1004 (2)	61 (3)	43 (3)	74 (3)	11 (2)	2 (2)	13 (2)
CR(66)	1528 (4)	3184 (3)	1276 (2)	46 (2)	40 (2)	41 (2)	10 (2)	4 (2)	1 (2)
CT(11)	9613 (8)	4302 (5)	9576 (4)	147 (6)	80 (4)	161 (7)	64 (4)	-23 (5)	3 (4)
CT(12)	8392 (15)	3832 (9)	9799 (7)	156 (13)	72 (8)	124 (11)	41 (8)	9 (9)	29 (8)
CT(13)	8014 (9)	4317 (6)	10517 (5)	159 (8)	121 (6)	232 (10)	65 (6)	28 (7)	46 (6)
CT(14)	9183 (17)	5249 (12)	10652 (7)	180 (15)	161 (14)	99 (10)	110 (12)	-14 (10)	18 (9)
CT(15)	9278 (14)	4770 (8)	10272 (6)	145 (11)	68 (7)	118 (10)	77 (8)	27 (8)	28 (6)
CT(21)	6280 (7)	191 (6)	5137 (3)	84 (5)	162 (7)	115 (6)	41 (4)	13 (4)	42 (5)
CT(22)	6189 (14)	-479 (11)	4568 (7)	124 (11)	143 (12)	119 (11)	51 (10)	58 (9)	81 (9)
CT(23)	5085 (11)	-997 (7)	4176 (5)	225 (11)	194 (9)	151 (8)	36 (8)	60 (7)	3 (7)
CT(24)	3779 (14)	-942 (13)	4309 (8)	77 (9)	200 (16)	138 (13)	28 (10)	9 (9)	23 (11)
CT(25)	5095 (18)	-303 (11)	4738 (6)	194 (14)	124 (12)	87 (10)	61 (11)	75 (10)	54 (9)

1.64 (2) Å, averaging 1.40 Å. The large variation in these distances should not be taken seriously; it only reflects the difficulties in treating the disorder with an independent atom model.

Tricyclohexylphosphine Geometry. The cyclohexyl rings are in the chair conformation. The absolute values of the endocyclic torsion angles vary from 50.7 to 58.9° with a mean of 55.8°, similar to the value of cyclohexane in the gas phase.⁸ The absolute values of only two such torsion angles are less than 53.2°; these are ω CR(56)–CR(51)–CR(52)–CR(53) and ω CR(52)–CR(51)–CR(56)–CR(55), -51.4 and 50.7°, re-

spectively. The relative flattening of ring 5 at CR(51) is also reflected in the angle CR(52)–CR(51)–CR(56), 112.7(3)°, which is the largest CR(J2)–CR(J1)–CR(J6) angle, the other five averaging 109.3 (5)°.⁹ The peculiarities of ring 5 may be the results of intramolecular repulsions, the atoms of this ring forming a number of short nonbonded contacts with atoms of other cyclohexyl groups and the anthracene ligand (Table V). The other 30 CR–CR–CR bond angles average 111.3 (6)°, the normal value for this parameter.⁸

The average CR–CR distance is 1.525 (12) Å, which compares well with the values found for other cyclohexyl

Table II. Final Atomic Coordinates ($\times 10^4$) and Final Thermal Parameters ($\times 100$) with Standard Deviations for Hydrogen Atoms

Atom	<i>x</i>	<i>y</i>	<i>z</i>	<i>U</i> _{iso}
H(1)	-2216 (34)	909 (24)	3082 (16)	4 (1)
H(2)	-712 (37)	1514 (26)	4084 (18)	5 (1)
H(3)	930 (42)	775 (30)	4434 (20)	7 (1)
H(4)	597 (37)	-892 (26)	4033 (17)	5 (1)
H(5)	-1998 (40)	-3885 (28)	2466 (19)	6 (1)
H(6)	-3804 (48)	-4685 (34)	1561 (23)	10 (2)
H(7)	-4986 (40)	-3708 (28)	1081 (19)	6 (1)
H(8)	-4628 (38)	-1982 (27)	1507 (18)	5 (1)
H(9)	-3482 (35)	-574 (25)	2303 (17)	5 (1)
H(10)	-766 (42)	-2474 (30)	3272 (19)	7 (1)
H(11)	1622 (30)	2624 (21)	4605 (14)	2 (1)
H(12A)	3225 (33)	4680 (23)	4820 (15)	3 (1)
H(12B)	3879 (33)	3802 (24)	4882 (16)	4 (1)
H(13A)	3296 (32)	4342 (23)	5920 (15)	3 (1)
H(13B)	2429 (36)	3175 (26)	5783 (17)	5 (1)
H(14A)	1455 (31)	4877 (22)	5694 (15)	3 (1)
H(14B)	955 (34)	4099 (24)	6213 (16)	4 (1)
H(15A)	-781 (35)	3701 (24)	5328 (16)	4 (1)
H(15B)	-209 (36)	2815 (25)	5411 (17)	5 (1)
H(16A)	-378 (38)	3174 (27)	4204 (17)	5 (1)
H(16B)	667 (29)	4278 (20)	4408 (14)	2 (1)
H(21)	2619 (32)	4187 (22)	2679 (15)	3 (1)
H(22A)	4135 (38)	5308 (27)	3570 (18)	6 (1)
H(22B)	2764 (37)	5459 (26)	3873 (17)	5 (1)
H(23A)	3719 (46)	6085 (33)	2626 (22)	9 (2)
H(23B)	3985 (41)	6810 (30)	3223 (19)	7 (1)
H(24A)	1961 (40)	6823 (28)	2579 (19)	6 (1)
H(24B)	1361 (43)	6424 (30)	3210 (20)	8 (1)
H(25A)	1187 (41)	5101 (29)	2101 (19)	7 (1)
H(25B)	-55 (38)	5237 (27)	2413 (18)	6 (1)
H(26A)	222 (35)	4415 (25)	3362 (16)	4 (1)
H(26B)	129 (33)	3690 (23)	2692 (15)	3 (1)
H(31)	4543 (31)	3831 (22)	3842 (14)	2 (1)
H(32A)	3683 (33)	1667 (24)	3660 (16)	4 (1)
H(32B)	3766 (32)	2260 (23)	4383 (15)	3 (1)
H(33A)	5792 (44)	1773 (32)	4182 (21)	8 (1)
H(33B)	6352 (39)	3002 (27)	4323 (18)	6 (1)
H(34A)	6042 (36)	1905 (26)	3001 (17)	5 (1)
H(34B)	7548 (37)	2618 (26)	3422 (17)	5 (1)
H(35A)	6767 (35)	3454 (25)	2576 (17)	5 (1)
H(35B)	6891 (33)	4120 (23)	3227 (15)	3 (1)
H(36A)	4559 (33)	3842 (23)	2640 (15)	4 (1)
H(36B)	4144 (40)	2570 (28)	2613 (19)	7 (1)
H(41)	-1785 (30)	335 (21)	1665 (14)	2 (1)
H(42A)	-1527 (36)	2430 (25)	1520 (17)	5 (1)
H(42B)	-1902 (31)	1883 (22)	2166 (14)	2 (1)
H(43A)	-4051 (39)	1934 (27)	1604 (18)	6 (1)
H(43B)	-4091 (37)	844 (26)	1679 (17)	5 (1)
H(44A)	-3364 (40)	1867 (28)	451 (19)	7 (1)
H(44B)	-4717 (50)	928 (35)	589 (23)	10 (2)
H(45A)	-3091 (38)	360 (26)	-61 (17)	5 (1)
H(45B)	-3441 (35)	-228 (25)	647 (17)	5 (1)
H(46A)	-903 (35)	413 (25)	541 (16)	4 (1)
H(46B)	-964 (35)	1553 (24)	483 (16)	4 (1)
H(51)	300 (32)	-251 (22)	2175 (15)	3 (1)
H(52A)	2611 (42)	688 (30)	2575 (19)	7 (1)
H(52B)	3112 (39)	686 (27)	1802 (18)	6 (1)
H(53A)	2134 (41)	-1095 (29)	2564 (19)	7 (1)
H(53B)	3568 (41)	-590 (29)	2381 (19)	7 (1)
H(54A)	2500 (43)	-2015 (30)	1603 (20)	7 (1)
H(54B)	3019 (47)	-957 (34)	1182 (22)	10 (2)
H(55A)	78 (43)	-1970 (30)	1597 (20)	7 (1)
H(55B)	530 (46)	-1991 (33)	852 (22)	9 (2)
H(56A)	1012 (39)	-250 (28)	865 (18)	6 (1)
H(56B)	-661 (42)	-820 (30)	1103 (20)	8 (1)
H(61)	2726 (39)	2456 (27)	1709 (18)	6 (1)
H(62A)	1512 (38)	1658 (27)	370 (18)	6 (1)
H(62B)	2602 (34)	1224 (24)	799 (16)	4 (1)
H(63A)	4007 (43)	2510 (30)	41 (20)	8 (1)
H(63B)	4478 (40)	2879 (28)	767 (19)	7 (1)
H(64A)	2461 (39)	3474 (27)	13 (18)	6 (1)
H(64B)	4043 (41)	4134 (29)	256 (19)	7 (1)
H(65A)	2479 (35)	4575 (24)	937 (16)	4 (1)
H(65B)	3624 (42)	4225 (30)	1399 (20)	7 (1)
H(66A)	1256 (37)	3432 (27)	1717 (18)	5 (1)
H(66B)	764 (34)	3009 (24)	928 (16)	4 (1)

Table III. Selected Bond Distances (Å) for (TCP)₂Ni(C₁₄H₁₀)·C₆H₅CH₃

Ni-P(1)	2.227 (1)	CR(31)-CR(32)	1.527 (6)
Ni-P(2)	2.241 (1)	CR(31)-CR(36)	1.535 (5)
Ni-C(1)	2.060 (4)	CR(32)-CR(33)	1.534 (6)
Ni-C(2)	1.993 (4)	CR(33)-CR(34)	1.503 (6)
		CR(34)-CR(35)	1.509 (6)
C(1)-C(2)	1.422 (6)	CR(35)-CR(36)	1.531 (6)
C(1)-C(12)	1.450 (5)	CR(41)-CR(42)	1.549 (6)
C(1)-H(1)	1.00 (3)	CR(41)-CR(46)	1.533 (5)
C(2)-C(3)	1.433 (6)	CR(42)-CR(43)	1.522 (6)
C(2)-H(2)	0.89 (4)	CR(43)-CR(44)	1.510 (6)
C(3)-C(4)	1.349 (6)	CR(44)-CR(45)	1.527 (7)
C(4)-C(11)	1.434 (6)	CR(45)-CR(46)	1.521 (6)
C(5)-C(6)	1.351 (7)	CR(51)-CR(52)	1.539 (6)
C(5)-C(14)	1.419 (6)	CR(51)-CR(56)	1.530 (6)
C(6)-C(7)	1.394 (7)	CR(52)-CR(53)	1.535 (7)
C(7)-C(8)	1.351 (7)	CR(53)-CR(54)	1.506 (7)
C(8)-C(13)	1.415 (6)	CR(54)-CR(55)	1.516 (8)
C(9)-C(12)	1.386 (5)	CR(55)-CR(56)	1.534 (6)
C(9)-C(13)	1.413 (6)	CR(61)-CR(62)	1.544 (5)
C(10)-C(11)	1.397 (6)	CR(61)-CR(66)	1.537 (6)
C(10)-C(14)	1.405 (6)	CR(62)-CR(63)	1.522 (6)
C(11)-C(12)	1.433 (5)	CR(63)-CR(64)	1.511 (7)
C(13)-C(14)	1.423 (6)	CR(64)-CR(65)	1.514 (7)
		CR(65)-CR(66)	1.529 (6)
P(1)-CR(11)	1.891 (4)		
P(1)-CR(21)	1.868 (4)	CT(11)-CT(12)	1.26 (2)
P(1)-CR(31)	1.863 (4)	CT(11)-CT(15)	1.58 (1)
P(2)-CR(41)	1.863 (4)	CT(11)-CT(14) ^a	1.25 (2)
P(2)-CR(51)	1.871 (4)	CT(11)-CT(15) [']	1.39 (1)
P(2)-CR(61)	1.872 (4)	CT(12)-CT(13)	1.64 (2)
		CT(13)-CT(14)	1.41 (2)
CR(11)-CR(12)	1.535 (5)	CT(13)-CT(15)	1.31 (2)
CR(11)-CR(16)	1.542 (5)	CT(21)-CT(22)	1.40 (2)
CR(12)-CR(13)	1.530 (5)	CT(21)-CT(25)	1.34 (2)
CR(13)-CR(14)	1.506 (6)	CT(21)-CT(24) ^{''}	1.49 (2)
CR(14)-CR(15)	1.515 (6)	CT(21)-CT(25) [']	1.44 (2)
CR(15)-CR(16)	1.517 (5)	CT(22)-CT(23)	1.28 (2)
CR(21)-CR(22)	1.528 (6)	CT(23)-CT(24)	1.35 (2)
CR(21)-CR(26)	1.531 (6)	CT(23)-CT(25)	1.43 (2)
CR(22)-CR(23)	1.522 (6)		
CR(23)-CR(24)	1.507 (8)		
CR(24)-CR(25)	1.508 (7)		
CR(25)-CR(26)	1.527 (7)		

^a Singly and doubly primed atoms are related to those of the asymmetric unit by $x', y', z' = 2 - x, 1 - y, 2 - z$ and $x'', y'', z'' = 1 - x, -y, 1 - z$, respectively.

groups bonded to a phosphorus atom¹⁰ and with that of cyclohexane itself.⁸ The spread in these distances appears to be too large, even if we increase our σ 's by 50%. Due to the C-P bonds, the cyclohexyl moieties have at most $C_s(m)$ symmetry with the following pairs of equivalent bonds: CR(J1)-CR(J2) and CR(J1)-CR(J6), CR(J2)-CR(J3) and CR(J6)-CR(J5), CR(J3)-CR(J4) and CR(J5)-CR(J4). The three unique distances average 1.536 (7), 1.527 (6), and 1.511 (6) Å, respectively. A comparison with the average σ 's of these bond lengths (Table III) shows that the C_s model describes the C-C distances to within the error of the individual values. The reason for the trend is not clear. Conceivably substituent effects could lead to a slight lengthening of the C-C bonds of CR(J1) while thermal motion might produce an apparent shortening in the bond lengths as found, particularly in those of CR(J4). Such proposals have been made to rationalize similar trends in C-C bond lengths of phenylphosphine compounds.¹¹

While the average P-C-H bond angle, 101.0 (28)^o, is small, the average H-CR-H and H-CR-CR bond angles are normal, 107.8 (42) and 109.2 (28)^o, respectively. The equatorial substitution of the cyclohexyl groups is shown by the average of the absolute value of the torsion angles ω P-CR(J1)-CR(J2)-CR(J3) and ω P-CR(J1)-CR(J6)-CR(J5), 171.6^o. The individual values are scattered from 166.5 to 177.9^o. The P-C-C bond angles also vary widely, 109.8 (3) to 120.9 (3)^o, with an average value of 115.3^o. The variation

Table IV. Selected Bond and Torsion Angles (deg)^a for (TCP)₂Ni(C₁₄H₁₀)·C₆H₅CH₃

P(1)-Ni-P(2)	118.3 (1)	C(8)-C(13)-C(9)	122.9 (4)
P(1)-Ni-C(2)	101.6 (1)	C(8)-C(13)-C(14)	118.4 (4)
P(2)-Ni-C(1)	101.7 (1)	C(9)-C(13)-C(14)	118.7 (4)
P(1)-Ni-C(1)	139.1 (1)	C(5)-C(14)-C(10)	123.4 (4)
P(2)-Ni-C(2)	139.7 (1)	C(5)-C(14)-C(13)	118.1 (4)
C(1)-Ni-C(2)	41.0 (2)	C(10)-C(14)-C(13)	118.6 (4)
Ni-C(1)-C(2)	66.9 (2)	Ni-P(1)-CR(11)	112.1 (1)
Ni-C(2)-C(1)	72.0 (2)	Ni-P(1)-CR(21)	114.2 (1)
Ni-C(1)-C(12)	119.9 (2)	Ni-P(1)-CR(31)	119.0 (1)
Ni-C(2)-C(3)	106.8 (3)	Ni-P(2)-CR(41)	111.6 (1)
Ni-C(1)-H(1)	103 (2)	Ni-P(2)-CR(51)	104.2 (1)
Ni-C(2)-H(2)	107 (2)	Ni-P(2)-CR(61)	121.5 (1)
C(2)-C(1)-H(1)	120 (2)	P(1)-CR(11)-CR(12)	119.6 (3)
C(1)-C(2)-H(2)	119 (2)	P(1)-CR(11)-CR(16)	112.4 (2)
C(12)-C(1)-H(1)	115 (2)	CR(12)-CR(11)-CR(16)	108.9 (3)
C(3)-C(2)-H(2)	120 (2)	CR(11)-CR(12)-CR(13)	109.7 (3)
C(12)-C(1)-C(2)	120.1 (3)	CR(12)-CR(13)-CR(14)	112.5 (3)
C(3)-C(2)-C(1)	117.4 (4)	CR(13)-CR(14)-CR(15)	111.3 (3)
C(2)-C(3)-C(4)	122.4 (7)	CR(14)-CR(15)-CR(16)	111.1 (3)
C(3)-C(4)-C(11)	121.6 (4)	CR(11)-CR(16)-CR(15)	111.5 (3)
C(14)-C(5)-C(6)	121.4 (4)	P(1)-CR(21)-CR(22)	118.4 (3)
C(5)-C(6)-C(7)	120.3 (5)	P(1)-CR(21)-CR(26)	113.4 (3)
C(6)-C(7)-C(8)	120.6 (5)	CR(22)-CR(21)-CR(26)	109.8 (3)
C(7)-C(8)-C(13)	121.3 (4)	CR(21)-CR(22)-CR(23)	111.2 (4)
C(12)-C(9)-C(13)	122.6 (4)	CR(22)-CR(23)-CR(24)	111.7 (4)
C(11)-C(10)-C(14)	122.4 (4)	CR(23)-CR(24)-CR(25)	111.0 (4)
C(4)-C(11)-C(10)	122.9 (4)	CR(24)-CR(25)-CR(26)	111.8 (4)
C(4)-C(11)-C(12)	118.2 (4)	CR(21)-CR(26)-CR(25)	111.3 (4)
C(10)-C(11)-C(12)	118.9 (4)	P(1)-CR(31)-CR(32)	111.5 (3)
C(1)-C(12)-C(9)	122.3 (3)	P(1)-CR(31)-CR(36)	114.2 (3)
C(1)-C(12)-C(11)	119.1 (3)	CR(32)-CR(31)-CR(36)	109.6 (3)
C(9)-C(12)-C(11)	118.7 (3)	CR(31)-CR(32)-CR(33)	111.1 (3)
P(2)-CR(41)-CR(42)	111.6 (3)	CR(32)-CR(33)-CR(34)	112.2 (4)
P(2)-CR(41)-CR(46)	120.5 (3)	CR(33)-CR(34)-CR(35)	111.1 (4)
CR(42)-CR(41)-CR(46)	108.7 (3)	CR(34)-CR(35)-CR(36)	111.3 (4)
CR(41)-CR(42)-CR(43)	111.0 (3)	CR(31)-CR(36)-CR(35)	111.3 (3)
CR(42)-CR(43)-CR(44)	111.4 (3)	CT(11)-CT(15)'-CT(11)'	107 (1) ^a
CR(43)-CR(44)-CR(45)	111.5 (4)	CT(11)'-CT(15)'-CT(13)'	118 (1)
CR(44)-CR(45)-CR(46)	111.2 (4)	CT(11)-CT(15)'-CT(13)'	134 (1)
CR(41)-CR(46)-CR(45)	110.3 (3)	CT(12)-CT(11)-CT(15)'	137 (1)
P(2)-CR(51)-CR(52)	109.8 (3)	CT(14)-CT(11)'-CT(15)'	117 (1)
P(2)-CR(51)-CR(56)	120.8 (3)	CT(11)-CT(12)-CT(13)	116 (1)
CR(52)-CR(51)-CR(56)	112.7 (3)	CT(12)-CT(13)-CT(14)	104 (1)
CR(51)-CR(52)-CR(53)	111.3 (4)	CT(13)-CT(14)-CT(11)'	138 (1)
CR(52)-CR(53)-CR(54)	111.7 (4)	CT(21)-CT(25)''-CT(21)''	122 (1)
CR(53)-CR(54)-CR(55)	110.8 (4)	CT(21)''-CT(25)''-CT(23)''	123 (1)
CR(54)-CR(55)-CR(56)	112.2 (4)	CT(21)-CT(25)''-CT(23)''	116 (1)
CR(51)-CR(56)-CR(55)	111.5 (3)	CT(22)-CT(21)-CT(25)''	112 (1)
P(2)-CR(61)-CR(62)	120.9 (3)	CT(21)-CT(22)-CT(23)	129 (1)
P(2)-CR(61)-CR(66)	110.7 (3)	CT(22)-CT(23)-CT(24)	119 (1)
CR(62)-CR(61)-CR(66)	109.5 (3)	CT(23)-CT(24)-CT(21)''	118 (1)
CR(61)-CR(62)-CR(63)	110.3 (3)	CT(24)-CT(21)''-CT(25)''	120 (1)
CR(62)-CR(63)-CR(64)	112.3 (4)		
CR(63)-CR(64)-CR(65)	111.6 (4)		
CR(64)-CR(65)-CR(66)	110.8 (4)		
CR(61)-CR(66)-CR(65)	111.1 (3)		
Torsion Angles			
Ni-C(1)-C(2)-C(3)	-100.0	C(2)-C(3)-C(4)-C(11)	-3.0
Ni-C(1)-C(2)-H(2)	99.8	C(3)-C(4)-C(11)-C(12)	4.0
C(12)-C(1)-C(2)-Ni	112.3	C(4)-C(11)-C(12)-C(1)	3.1
H(1)-C(1)-C(2)-Ni	-92.2	C(2)-C(1)-C(12)-C(11)	-11.3
C(12)-C(1)-C(2)-C(3)	12.3		
C(1)-C(2)-C(3)-C(4)	-5.2		

^a See the footnote in Table III.

of the P-C bond lengths is probably significant, but their average value of 1.871 (10) Å compares well with those of P-C (cyclohexyl) in other compounds.¹⁰ The C-P-C bond angles do vary significantly from their mean of 104.7°. Apparently deformations of those TCP torsion and valency angles involving the phosphorus atoms are the mechanism chosen to relieve intramolecular steric strain in this part of the molecule. This observation is not surprising not only because the P atoms are near the middle of the molecule but also because the P-C

bonds are weaker than the C-C and C-H bonds and thus easier to deform.

The Ni atom forms bonds with P(1), 2.227 (1) Å, P(2), 2.241 (1) Å, C(1), 2.060 (4) Å, and C(2), 1.993 (4) Å. If the C(1)-C(2) bond is assigned one coordination site, then the coordination geometry of the Ni atom is trigonal. Thus this compound may be compared with other 16-electron Ni(0) structures. The mean Ni-C bond distance, 2.03 Å, is at the long end of the range of Ni-C bond lengths (1.91-2.02 Å)

Table V. Short Intramolecular Distances (Å) between the Ligands

C(2)-CR(11)	3.360 (6)	H(2)-H(16A)	2.22 (5)
C(9)-H(41)	2.52 (3)	H(9)-H(41)	2.21 (4)
C(11)-H(51)	2.67 (3)	CR(26)-H(66A)	2.81 (4)
C(12)-H(51)	2.63 (3)	H(21)-H(66A)	2.27 (5)
H(1)-H(42B)	2.29 (4)	H(26B)-H(66A)	2.33 (5)
H(2)-CR(11)	2.88 (4)	H(36B)-H(61)	2.20 (5)
H(2)-CR(16)	2.82 (4)		

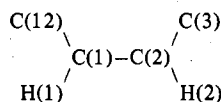
reported for $L_2Ni(\text{olefin})$ complexes, $L = \text{phosphine ligand}$.¹⁰

The differences in the two Ni-C bond lengths, 0.067 (6) Å, and the two Ni-P bond distances, 0.014 (2) Å, are significant. As is often observed in transition metal structures, the shorter bonds are trans (in this case pseudotrans) to the longer bonds. Since the molecule has no symmetry, we cannot rule out an electronic effect for the bond length difference; however, steric repulsion between the TCP ligand of P(2) and the anthracene moiety is the probable cause.

The Ni-P distances and P-Ni-P angle, 118.3 (1)°, observed here are both larger than those observed in $L_2Ni(\text{olefin})$ compounds. Several of these compounds have Ni-P distances of about 2.16 Å,¹⁰ and the largest P-Ni-P angle was determined in $[P(\text{OC}_6\text{H}_4\text{CH}_3)_3]_2Ni(\text{C}_2\text{H}_4)$, 116.3 (2)°.¹² The larger values observed here probably are due to the steric bulk of the TCP and anthracene ligand rather than to electronic effects since in $[(\text{C}_6\text{H}_{11})_2\text{PCH}_2\text{CH}_2\text{P}(\text{C}_6\text{H}_{11})_2]Ni[\text{C}_2(\text{CH}_3)_4]$ the Ni-P bond lengths are much shorter (average 2.156 (6) Å). Two TCP ligands should be electronically similar to $(\text{C}_6\text{H}_{11})_2\text{PCH}_2\text{CH}_2\text{P}(\text{C}_6\text{H}_{11})_2$ but sterically bulkier due to the chelate nature of the latter. Short Ni-P (2.18 (2) Å) and larger $\angle\text{P-Ni-P}$ (128 (1)°) were observed in the "end-on" bonded dinitrogen complex $\mu\text{-N}_2[Ni(\text{TCP})_2]_2$,¹³ which is consistent with the smaller steric size of a nitrogen atom compared to 1,2- $\eta\text{-C}_{14}\text{H}_{10}$. If we define a phosphorus threefold axis as a sum of the three P-C bond vectors, the angle formed by these threefold axes is 130.0°, which is 11.7° larger than P-Ni-P. Apparently the steric repulsions (Table V) between the two TCP ligands are relieved not only by the large $\angle\text{P-Ni-P}$ but also by a bending of the TCP ligands away from each other with the P atoms acting as the pivot centers. The nonlinearity of the Ni-P bonds with their associated phosphorus threefold axes is reflected in the variation of $\angle\text{Ni-P-C}$, 104.2 (1)-121.5 (1)°.

The Ni, P(1), P(2), C(1), C(2) fragment is not planar. The C(1)-C(2) bond axis forms an angle of 22.0° with the Ni, P(1), P(2) plane. The deviations of C(1) and C(2) from this plane are -0.316 (4) and 0.217 (5) Å, respectively. Distortions from nonplanarity have been noted in $L_2Ni(\text{olefin})$ structures, and its significance has been a subject of controversy. Recently we suggested that the 16.5° out-of-plane rotation observed in $[(\text{C}_6\text{H}_{11})_2\text{PCH}_2\text{CH}_2\text{P}(\text{C}_6\text{H}_{11})_2]Ni[\text{C}_2(\text{CH}_3)_4]$, one of the larger of such distortions reported, might be due to interligand steric interactions.¹⁰ Examination of molecular plots and interatomic distances revealed that the distortion observed here relieves in particular repulsions between anthracene atoms and cyclohexyl group 5. The anthracene moiety is forced away from the P(2) ligand as is shown by the 72.4° angle formed by the vector P(2)-P(1) with the normal to the least-squares best plane of the aromatic species (Table VI).¹⁴

Anthracene Geometry. The fragment



is nonplanar. The C(1)-C(2) bond axis forms angles of 70 and 72° with the normals to the planes C(1), H(1), C(12) and C(2), H(2), C(3) respectively. Since all torsion angles about C(1)-C(2) involving the nickel atom (Table IV) are either greater than 90° or less than -90°, clearly the substituents

Table VI. Best Weighted^a Least-Squares Planes for $(\text{TCP})_2Ni\text{C}_{14}\text{H}_{10}\cdot\text{C}_6\text{H}_5\text{CH}_3$

Equation ^b of the Plane	
1.	$-0.6356x - 0.3294y + 0.6982z - 5.5067 = 0.0$
2.	$-0.6256x - 0.3338y + 0.7051z - 5.5383 = 0.0$
3.	$-0.6330x - 0.3476y + 0.6917z - 5.5489 = 0.0$

Deviation (Å) of the Atoms from the Plane

- Ni,^c -1.8222 (5); P(1),^c -2.426 (1); P(2),^c -3.396 (1); C(1), -0.103 (4); C(2), 0.073 (4); C(3), 0.052 (5); C(4), -0.023 (5); C(5), 0.001 (5); C(6), -0.021 (6); C(7), -0.018 (5); C(8), 0.015 (5); C(9), 0.050 (4); C(10), -0.011 (4); C(11), -0.023 (4); C(12), -0.029 (4); C(13), 0.038 (4); C(14), 0.010 (4); H(1),^c 0.08 (3); H(2),^c 0.44 (4); H(3),^c 0.06 (4); H(4),^c 0.02 (4); H(5),^c 0.00 (4); H(6),^c 0.00 (5); H(7),^c -0.13 (4); H(8),^c -0.08 (4); H(9),^c 0.06 (3); H(10),^c 0.10 (4)
- C(5), 0.013 (5); C(6), -0.021 (6); C(7), -0.035 (5); C(8), -0.008 (5); C(9), 0.033 (4); C(10), 0.007 (4); C(11), -0.010 (4); C(12), -0.034 (4); C(13), 0.027 (4); C(14), 0.016 (4)
- C(5), 0.009 (5); C(6), 0.002 (6); C(7), -0.006 (5); C(8), 0.000 (5); C(13), 0.007 (4); C(14), -0.010 (4)

^a The weight of each atom was taken as $1/\sigma_{\perp}^2$, where σ_{\perp}^2 is the variance of the atom along the normal to the plane. ^b The direction cosines of the plane normal are given for a Cartesian cell with x along a , y perpendicular to a and in the ab plane, and z along c .

^c This atom was not included in the plane calculation.

of C(1) and C(2) are bent away from the metal atom. The average bending back angle (19 (1)°) is in the range reported for nickel-olefin compounds, 8 (2)° in *all-trans*-1,5,9-cyclododecatrienickel(0)¹⁵ to 42° in tetrafluoroethylene-(1,1,1-tris(diphenylphosphinomethyl)ethane)nickel(0).¹⁶

A novel feature is the torsion angle $\omega\text{C}(12)\text{-C}(1)\text{-C}(2)\text{-C}(3)$, 12.3°, which would be 0° if these four atoms were coplanar. The torsion angle is the largest observed to date for a cis-substituted unsaturated hydrocarbon that is 1,2-dihapto bonded to a metal atom. From an examination of the torsion angles about C(1)-C(2) involving the Ni atom, one may conclude that the nonplanarity of the C(12)-C(1)-C(2)-C(3) fragment arises from a rotation of the substituents of C(1) about the C(1)-C(2) axis in such a fashion that H(1) is moved toward the Ni atom while C(12) is moved in the opposite direction. Because the absolute values of $\omega\text{Ni-C}(1)\text{-C}(2)\text{-C}(3)$, 100.0°, and $\omega\text{Ni-C}(1)\text{-C}(2)\text{-H}(2)$, 99.8°, are essentially equal, no such rotation can be detected for the C(2) substituents. From these two observations we conclude that the 12.3° torsion angle does not reflect a desire of C(1) and C(2), which lie on the opposite sides of the Ni, P(1), P(2) plane, to incline their $p\pi$ orbitals in the direction of this Ni coordination plane. This fact indicates that the Ni atom shows no overwhelming desire to form all of its bonds in one plane, an observation that is consistent with current views of the nickel-olefin bond in trigonal nickel compounds.¹⁷ Noting that C(1) and C(2) show the largest positive and negative deviations from the plane of the anthracene species, that C(1) puckers out of this plane toward the Ni atom, and that the anthracene ligand slopes away from P(2) (Table VI), we suggest that the nonzero $\omega\text{C}(12)\text{-C}(1)\text{-C}(2)\text{-C}(3)$ may be caused by a minimization of the C(1)-Ni distance with a minimal increase in interligand nonbonded repulsions.

That Ni-C(1) is 0.067 (6) Å longer than Ni-C(2) indicates that other forces are working against increased nonplanarity, perhaps conjugation. The type of nonplanarity observed probably would not seriously disrupt anthracene conjugation. However, χ^2 tests show that the anthracenic C-C bond lengths observed here deviate significantly from those of free anthracene (Figure 3),¹⁸ even if C(1)-C(2) is ignored. Bond C(1)-C(2) is 0.047 (6) Å longer, C(2)-C(3) is 0.015 (6) Å longer, and C(3)-C(4) is 0.026 (6) Å shorter than the values found in the free ligand. These differences indicate a partial localization of the electrons in the C(1)-C(2)-C(3)-C(4) fragment to form a 1,3-butadiene-like species, the increase of

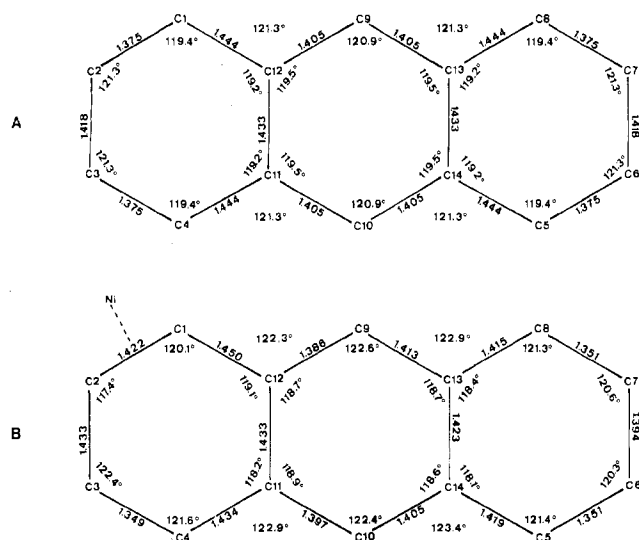


Figure 3. Bond distances and angles in free anthracene (A)¹⁸ and in the coordinated ligand B found in this study.

the C(1)–C(2) distance being due to the interaction with the Ni atom.

η^2 -Arene–Metal Bonding. If a double bond is fixed at C(1)–C(2), Ni/arene interaction may be described by the Dewar and Chatt scheme for the bonding of olefins to metal atoms. A three-center σ bond is formed by the filled olefinic π orbital and an empty metal orbital, and a three-center π bond is formed by a filled metal d orbital and an empty olefinic π^* orbital.¹⁹ Ignoring heats of solution, we may approximate the heat of formation of $L_2Ni(C_{14}H_{10})$, ΔH_{Ni-Ar} , as the enthalpy of nickel–olefin bond formation (ΔH_{Ni-C2}) minus the loss of resonance energy (ΔE_r) caused by localization of a double bond at C(1)–C(2). The latter is the difference in the resonance energy of anthracene and 2-vinylnaphthalene, which is the conjugated hydrocarbon obtained if the bond C(1)–C(2) of anthracene is removed from conjugation with the other carbon atoms. From simple Hückel theory the π resonance energy of anthracene and 2-vinylnaphthalene is 5.31 β and 4.11 β , respectively. For a β of 20 kcal/mol,²⁰ $\Delta E_r = 1.20 = 24$ kcal/mol. This value should be the upper limit for ΔE_r . We find evidence for only a *partial* localization in the anthracene bond lengths; therefore, after complex formation only a *partial* reduction of the resonance between the 2-vinylnaphthalene and C(1)–C(2) entities has occurred.

2-Vinylnaphthalene is the compound of highest resonance energy that may be derived from anthracene by removal of two adjacent carbon atoms. Thus the stereochemistry of the L_2Ni /anthracene interaction is consistent with the above outlined energetics. Similar reasoning may be applied to other cases in which the 1,2-dihapto interaction of a transition metal atom with a conjugated hydrocarbon causes a fixation in the C–C bond distances. Then we would expect that the metal atom interacts with that C–C bond which leaves the ligand with the highest resonance energy.

Applications to Related Systems

Examples of localization of arene bond lengths in tetrahapto complexes of $Fe(CO)_3$, $(\eta^6\text{-naphthalene})Cr(CO)_3$, and $(\eta^3\text{-benzyl})(\eta\text{-C}_5\text{H}_5)Mo(CO)_3$ have been discussed.²² Of particular interest here is the fact that α -vinylnaphthalene and β -vinylnaphthalene both form 1,2,11,12-tetrahapto complexes rather than 1,9,11,12-tetrahapto or 1,3,11,12-tetrahapto complexes, respectively, with $Fe(CO)_3$. Since the Hückel resonance energy of styrene (2.42 β) is larger than that of 1,3,5,7-octatetraene (1.52 β) or that of *o*-quinoline (1.95 β), the 1,2,11,12-tetrahapto structures are energetically more favorable. In the acenaphthylene compound of $Fe(CO)_4$,

five-membered ring carbon atoms, C(1) and C(2), form the bonds to the iron atom;²³ therefore, only a minimal loss of polyene resonance energy occurs. Since the difference in the resonance energy of benzene (2 β) and 1,3-butadiene (0.47 β) is large, it is not surprising that only one example of a 1,2- η^2 -benzene complex has been reported in which fixation of the C–C bond lengths is claimed, 1,2- η^2 - $C_6(CF_3)_6Pt[(C_2H_5)_3]$.²⁴ Probably the CF_3 groups stabilize this structure by lowering the resonance energy of the six-membered ring.

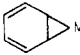
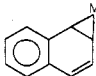
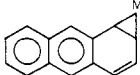
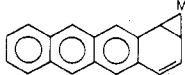
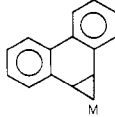
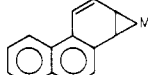
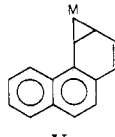
The best characterized class of 1,2-dihaptoarene/transition metal complexes is that of the silver(I) salts.²⁵ In comparison to the above cited arene/metal(0) compounds, the arene/ Ag^+ interaction is generally regarded as weak. For example, despite the fact that in anthracenetetrakis(silver perchlorate) monohydrate each C(1)–C(2) type bond is linked dihapto to a silver cation, these C–C bond lengths average 1.366 (9) Å, one standard deviation *shorter* than that found in anthracene itself (Figure 3A). It is possible that the interaction with the cation tends to localize the C(1)–C(2) type bonds but that Ag^+ lacks the back-bonding strength to lengthen the “fixed” double bonds. The long C(2)–C(3) bond, 1.487 (12) Å, in the silver complex does offer some slight evidence for such an effect. For this class of compounds, Fukui et al. used perturbation theory to predict not only which pair of arene carbon atoms would interact with the cation but also the relative stabilities of the complexes formed. It is reasoned that the energy of complex formation E is the increase in delocalization energy that occurs when arene electron density is donated to the silver cation. Fukui's LCAO–MO treatment indicated that E would be a function of

$$-\sum_{j=1}^f \frac{(c_r^j + c_s^j)^2}{h - \lambda_j}$$

if $h \neq \lambda_j$ and of $|C_r^j + C_s^j|$ if $h \neq \lambda_j$, where C_r^j and C_s^j are the coefficients of the atomic orbitals of C(r) and C(s), respectively (carbon atoms which bond to the cation), in the j th occupied molecular orbital of the arene, λ_j is the energy of the j th molecular orbital, h is the Coulomb energy of the silver cation, and f is the number of electrons in the highest occupied arene MO.^{26,29} The structural predictions made by this method agree well with those made above by consideration of ΔE_r upon complex formation. This is gratifying since the former only treats cases in which the perturbation of the arene by the metal atom is small while the latter presupposes a large interaction.

Both treatments assume, however, that 1,2-dihapto complexes would be formed. At the outset of this investigation, the mode of the L_2Ni (arene) interaction was not obvious. In addition to 1,2-dihapto bonding leading to a coordinatively unsaturated 16-electron complex, other π complexes with 1,2,3,4-tetrahapto (leading to 18-electron complexes) and 1,2,3,4,11,12-hexahapto (leading to coordinately supersaturated 20-electron complexes) stereochemistries could not be ruled out. A σ complex with the Ni atom bonding to C(9) and C(10) also had to be considered. Now that the structure is known and that the steric requirements of the TCP ligand have been detailed, other structures appear to be sterically too crowded to compete energetically with the 1,2-dihapto geometry. Assuming that the L_2Ni (arene) complexes reported¹ all contain 1,2-dihapto interactions and that fixation of the C–C bond lengths occurs, we have listed the most probable structures and have given the value of ΔE_r in units of β in Table VII. The structural predictions should be more reliable for the naphthalene and tetracene complexes since the interligand repulsions should be essentially identical to those of the anthracene compound. In the case of benzene a 1,2,3,4-tetrahapto geometry might be sterically possible. In the case of phenanthrene, the sterically more favorable 1,2-dihapto geometry Vb must be considered in addition to the

Table VII. Resonance Energies for 1,2-Dihapto Bond Arenes

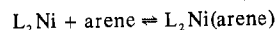
Complex	Resonance energy ^a of		ΔE_r
	Free arene	1,2-Dihapto-arene	
 I	2 ^b	0.47 ^b	1.53 ^b -30.6 ^c
 II	3.68	2.42	1.26-25.2
 III	5.31	4.11	1.20-24.0
 IV	6.87	5.74	1.13-22.6
 V _a	5.45	4.38	1.07-21.4
 V _b	5.45	4.13	1.32-26.4
 V _c	5.45	4.11	1.34-26.8

^a All energies are taken from simple Hückel calculations as described in the text. ^b These energies are given in terms of the parameter β .²¹ ^c These energies are given in kcal/mol assuming $\beta = 20$ kcal/mol.

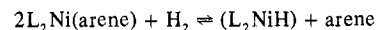
electronically favored 9,10-dihapto structure V_a.

Ni(arene) Reactivity

If the NiC₂ interactions vary little in strength and if the change in entropy for the reaction



is similar for each arene, then the smaller the value of ΔE_r , the greater the relative stability of the complex. The ease of replacement of benzene by the higher arenes¹ is then simple to understand. The observation that the equilibrium



lies further to the right for benzene than for naphthalene¹ also finds an explanation in the ΔE_r values.

If β is taken as 20 kcal/mol, one notes that the ΔE_r terms vary from 30 kcal/mol in I to 21.3 kcal/mol in V_a. Clearly all of the complexes are unstable to replacement of arene by ethylene. However, the ΔE_r values seem very large compared to recent estimates of various Ni-olefin bond strengths, 25-42

kcal/mol.²⁸ We mentioned earlier that the ΔE_r values are only upper limits since the localization of arene π density in the complexes is only partial. Therefore the relative magnitudes of the ΔE_r values are probably more important than are the quantitative values.

Registry No. (TCP)₂(C₁₄H₁₀)Ni-C₆H₅CH₃, 61332-70-5.

Supplementary Material Available: Listing of structure factor amplitudes (38 pages). Ordering information is given on any current masthead page.

References and Notes

- (1) K. Jonas, *J. Organomet. Chem.*, **78**, 273 (1974).
- (2) In addition to several local programs, local DEC-SYSTEM-10 versions of other programs used were: S. Lawton's TRACER for reduced cell calculations, Coppen's DATAP for calculations of $|F_o|$ and $\sigma(F_o)$, Sheldrick's SHEL-X programs for Fourier calculations and initial least squares, Sparks-Trueblood's block diagonal least-squares program, Davis' DAESD for bond distance and angle calculations, Roberts' XANADU program for geometrical calculations, Hirschfeld's ORTHO for best weighted least-squares plane calculations, and Johnson's ORTEP for the molecular drawings.
- (3) Numbers in parentheses following numerical values are the estimated standard deviation in the least significant digit.
- (4) (a) D. T. Cromer and J. T. Waber, *Acta Crystallogr.*, **18**, 104 (1965); (b) R. F. Stewart, E. R. Davidson, and W. T. Simpson, *J. Chem. Phys.*, **42**, 3175 (1965).
- (5) D. T. Cromer and D. Liberman, *J. Chem. Phys.*, **53**, 1891 (1970).
- (6) X-ray diffraction determinations of the C-H bond length are typically smaller than the true, equilibrium C-H separation of about 1.10 Å.⁷
- (7) M. R. Churchill, *Inorg. Chem.*, **12**, 1213 (1973).
- (8) H. R. Buys and H. J. Geise, *Tetrahedron Lett.*, **34**, 2991 (1970), and references cited therein.
- (9) Standard deviations given with average values are the larger of the mean of the errors derived from the least-squares σ 's or $(\sum_i^n (l_i - \bar{l})^2 / (n - 1))^{1/2}$, where n is the number of values averaged.
- (10) D. J. Brauer and C. Kruger, *J. Organomet. Chem.*, **77**, 423 (1974).
- (11) A. Domenicano and A. Vaciago, *Acta Crystallogr., Sect. B*, **31**, 2553 (1975).
- (12) L. J. Guggenberger, *Inorg. Chem.*, **12**, 499 (1973).
- (13) P. W. Jolly, K. Jonas, C. Kruger, and Y.-H. Tsay, *J. Organomet. Chem.*, **33**, 109 (1971).
- (14) In an undistorted molecule, this angle would be 90°.
- (15) D. J. Brauer and C. Kruger, *J. Organomet. Chem.*, **44**, 397 (1972).
- (16) J. Browning and B. R. Penfold, *J. Chem. Soc., Chem. Commun.*, 198 (1973).
- (17) N. Rosch and R. Hoffmann, *Inorg. Chem.*, **13**, 2656 (1974).
- (18) R. Mason, *Acta Crystallogr.*, **17**, 547 (1964).
- (19) M. J. S. Dewar, *Bull. Soc. Chim. Fr.*, **18**, 79 (1951); J. Chatt and L. A. Duncanson, *J. Chem. Soc.*, 2939 (1953).
- (20) For a discussion of the difficulties associated with the value of β , see ref 21.
- (21) A. Streitwieser, "Molecular Orbital Theory for Organic Chemists", Wiley, New York, N.Y., 1961, pp 246 and 247.
- (22) R. E. Davis and R. Pettit, *J. Am. Chem. Soc.*, **92**, 716 (1970).
- (23) F. A. Cotton and P. Lahuerta, *Inorg. Chem.*, **14**, 116 (1975).
- (24) J. Browning, M. Green, B. R. Penfold, J. L. Spencer, and F. G. A. Stone, *J. Chem. Soc., Chem. Commun.*, 31 (1973).
- (25) E. A. H. Griffith and E. L. Amma, *J. Am. Chem. Soc.*, **96**, 5407 (1974), and references cited therein.
- (26) K. Fukui, A. Imamura, T. Lonzawa, and C. Nagata, *Bull. Chem. Soc. Jpn.*, **34**, 1076 (1961).
- (27) W. E. Rhine, J. Davis, and G. Stucky, *J. Am. Chem. Soc.*, **97**, 2079 (1975).
- (28) C. A. Tolman, *J. Am. Chem. Soc.*, **96**, 2780 (1974).
- (29) In general one cannot modify the Dewar and Chatt bonding scheme by replacing the olefin π and π^* orbitals with the arene HOMO (highest occupied molecular orbital) and arene LUMO (lowest unoccupied molecular orbital), respectively. First the HOMO of anthracene is bonding not only at C(1), C(2) but also at C(3), C(4), at C(5), C(6), and at C(7), C(8). Second the anthracene LUMO is antibonding with respect to each of these four bonds. Removal of electrons from the anthracene HOMO and addition of electrons to the anthracene LUMO must then lead to a lengthening of each of these four bonds. This prediction is contrary to observation: only C(1)-C(2) is lengthened, the other three bonds show a shortening. Clearly the geometry of the anthracene found here does not correspond to that of anthracene in its lowest excited state. This observation is in contrast to those made for dilithium salts of naphthalene and anthracene in which the geometries of the arene dianions presumably correspond to those of the arene in its lowest excited state.²⁷ The difference between arene/dilithium and anthracene/nickel compounds is probably due to the more specific nature of the anthracene/nickel interaction (the arene/dilithium interactions involve more carbon atoms) as well as the more ionic nature of the arene/dilithium bond.